Jan Jedelský

SOME ASPECTS OF EFFERVESCENT ATOMIZATION: EXPERIMENTAL STUDY

Brno University of Technology
Faculty of Mechanical Engineering
Energy Institute

Ing. Jan Jedelský, Ph.D.

**SOME ASPECTS OF EFFERVESCENT ATOMIZATION:
EXPERIMENTAL STUDY**

EXPERIMENTÁLNÍ STUDIE NĚKTERÝCH ASPEKTŮ SPREJŮ
TYPU „EFFERVESCENT"

Short version of Habilitation Thesis
Zkrácená verze habilitační práce

Specialization: Design and Process Engineering

VUTIUM

Brno, 2013

KEY WORDS

two-phase flow, effervescent atomization, spray characteristics, suspensions, gas–liquid mixture, atomization efficiency

KLÍČOVÁ SLOVA

dvoufázové proudění, effervescent atomizace, vlastnosti spreje, suspenze, směs kapalina–plyn, atomizační účinnost

MÍSTO ULOŽENÍ PRÁCE

Oddělení pro vědu a výzkum Fakulty strojního inženýrství Vysokého učení technického v Brně.

TABLE OF CONTENTS

AUTHOR'S CURRICULUM VITAE

Ing. Jan JEDELSKÝ, Ph.D.

Born: 19. 7. 1971 in Valašské Meziříčí

Education and academic qualification:
- 1994, Master of Science, Brno University of Technology, Faculty of Mechanical Engineering, specialization: Transport Engineering
- 2002, Ph.D., Brno University of Technology, Faculty of Mechanical Engineering, specialization: Design and Process Engineering

Career overview:
- 1994–1997, PhD studies, Dpt. of Internal Combustion Engines and Vehicles, BUT Brno
- 1997–2001, assistant, Institute of Automotive Engineering, Dpt. of IC Engines, BUT Brno
- 1997–present, assistant, further assistant to professor, Brno University of Technology, Faculty of Mechanical Engineering

Pedagogic activities:
- Co-author of 3 hypertext textbooks
- 1997–1998, tutorial of Combustion engine testing (5th year)
- 1998–present, guidance of 16 Diploma Thesis
- 1999–2001, tutorial of Year-class project (5th year)
- 2000–2002, tutorial of Year-class project (4th year)
- 2001–2002, tutorial of Combustion engine theory (4th year)
- 2001–2003, lectures & tutorial of Propulsions and Engines (3rd year)
- 2002–present, guidance of 8 Bachelor Thesis
- 2004–present, tutorial of Thermomechanics
- 2005–present, supervisor/specialist in Ph.D. study (2x Ph.D)

Scientific activities:
- 1994–1998, Stirling engines (utilization for solar energy conversion, low-temperature SE)
- 1995–2001, SI combustion engines (noise and vibrations sources, crankshaft dynamics)
- 1998–present, experimental fluid dynamics of single- and multi-phase flows (atomization, internal gas-liquid flows; application of laser diagnostic methods PIV–PLIF, PDA
- 2007–present, transport and deposition of particles in human airways
- Cooperation within 18 grant projects (GAČR, EUREKA, COST, FRVŠ, KONTAKT)
- Three Czech national patents, two utility models
- Five IF papers (20 citations according SCI), 10 papers indexed in WoS , 45 conference papers

University and non-university activities:
- 1999–2005, Member of the Faculty academic senate FME BUT Brno
- 2002–present, Member of ILASS Europe,
- 2011–present, Committee member of ILASS Europe
- 2009 Member of Czech Aerosol Society
- 2007–present, reviewer of 12 international impacted journals

NOMENCLATURE

A = cross-section area (m^2)

a = specific surface area

a, b = coefficients (in chapter 4.2)

a_e = specific expansion work

C = mass concentration (kg/m^3)

C_d = discharge coefficient

c = specific heat capacity (J/kg·K)

D = droplet (particle) diameter (μm)

D_{20} = surface area mean diameter (μm)

D_{32} = Sauter Mean Diameter (μm)

D_{pq} = mean drop diameter with indices p and q used for determination of the diameter (μm)

D_{va} = mean drop diameter representing a drop size bellow which volumetric fraction a of total droplet volume occurs, usually a = 0.1, 0.5 or 0.9 (μm)

d_a = diameter of air injection holes (mm)

d_c = diameter of the mixing chamber (mm)

d_o = diameter of the final discharge orifice (mm)

E = energy (J)

e = specific energy

f = droplet arrival frequency (data rate) (Hz)

$f_a(D)$ = frequency distribution of drops, a = 0 refers to the number distributions, a = 2 to the surface distributions and a = 3 to the volume distributions

G = mass velocity (mass flux density) (kg/m^2·s)

GLR = gas-to-liquid mass flow rate ratio (%, –)

ID_{32} = Integral Sauter Mean Diameter (μm)

i = specific enthalpy

J = total momentum of a jet

K = isentropic exponent of the two-phase mixture

k = gas isentropic exponent

l = distance, length (characteristic dimension of the measurement volume) (m)

l_c = length downstream of the last row of air holes, mixing chamber length (mm)

l_o = length the final discharge orifice (mm)

m = number of droplets in given measurement position (in chapter 4.2)

$\dot{m}$ = mass flow rate (kg/s, g/s)

N_a = number of aeration holes

n = number of drops measured by PDA, number of measurement positions

n_r = index of refraction

p = pressure (Pa)

q = specific heat

r = radial position in the spray (m)

t = time, time period of measurement (s)

V = volume (m^3)

v = velocity (m/s)

w = axial velocity (m/s)

X, Y = Cartesian coordinates, coordinates of two-phase flow map

x, y, z = Cartesian coordinates

Z = vertical coordinate (m)

Greek Symbols

β = half-angle of the flow convergence downstream of the mixing chamber (degrees)

Δl = span length between the first and the last set of aeration holes (mm)

Δp = pressure differential between the mixing chamber and ambient air (Pa, MPa)

Δp_{gl} = pressure differential between gas and liquid at atomizer inlet (kPa)

Δr = distance between adjacent measurement points (m)

η_a = atomization efficiency

κ = gas isentropic exponent

μ = dynamic viscosity (N·s/m^2)

ρ = density (kg/m^3)

σ = liquid/gas surface tension (N/m)

$\Phi_a(D)$ = cumulative distribution of drops, $a = 0$ refers to the number distributions, $a = 2$ to the surface distributions and $a = 3$ to the volume distributions

Subscripts

1 = in the atomizer mixing chamber

2 = at the atomizer exit (ambient air conditions)

a = air, surface area in chapter 5

b = bubble

d = droplet

g = atomizing gas, usually air

i, j = index number

k = kinetic energy

l = atomized liquid

m = two-phase mixture

$mean$ = mean value

p = at constant pressure

v = at constant volume

w = water

Superscripts

$(\ )'$ = fluctuating value

$(\ \bar{}\ )'$ = root-mean-squared fluctuating value

$(\ \bar{}\ )$ = mean value, time-averaged mean value

$\overline{\hat{C'}}$ = root-mean-squared fluctuating value of a quantity C normalised by its mean value $\overline{C}$

1 INTRODUCTION

Presented text systematically summarises my effort dedicated to the effervescent atomization. It is based on experimental findings acquired at the Energy department, FME BUT during past 14 years.

1.1 PREFACE

Original motivation of the work was to design an effervescent atomizer for light heating oil (LHO) spraying to replace pressure-swirl atomizers in retrofits of industrial burners. We consequently solved several demands for waste liquid and suspension atomization where effervescent atomization was found to be a suitable method. Going more deeply into basic processes related to internal twin-fluid atomization we have realised it to be very complex and not well studied topic yet. For example a relation of the internal flow to spray characteristics, flow field in the spray and a problem of spray unsteadiness.

Realisation of these research works would not be possible without a financial support, namely from the Ministry of Education of the Czech Republic through the project Eureka E! 2517 BURNER, from Brno University Research Plan No. MSM262100001 and the projects GA 101/03/P020, GA 101/06/0750 and GA 101/11/1264 funded by the Czech Science Foundation. The work was done by myself, often in collaboration and support from my supervisor prof. Jícha, colleague ing. Sláma (First Brno Engineering Works) and students of our department. Some parts of these works were published in conference and journal papers.

The work is focused on experimental investigation of a single-hole, plain-orifice effervescent atomizer with an "outside-in" gas injection configuration for combustion applications. The first part of the work is focused on internal two-phase flow. In the next part spray characteristics are investigated using Particle Image Velocimetry – Planar Laser-Induced Fluorescence (PIV–PLIF) technique and by means of Phase-Doppler Anemometry (PDA). Energy considerations in effervescent atomization in following chapter result in an estimation of atomization efficiency. One of the goals of our work was a development of a new procedure for the design of effervescent atomizers. The last chapter describes several applications of the effervescent atomizer for waste fuel and suspension spraying and introduces several novel designs of pneumatic atomizers.

1.2 EFFERVESCENT ATOMIZATION

Atomization is a process of conversion of bulk liquid into small drops thus increasing the ratio of surface area to volume. It requires an external energy to overcome surface tension forces and it can be carried out by a variety of means: aerodynamically, mechanically, ultrasonically, or electrostatically [1]. Bayvel and Orzechowski [2] classify atomizers based on atomization energy type used (liquid pressure, gas pressure, mechanical energy, vibrational energy, electric energy, etc.).

Pressure atomizers, as the most common type of atomizing device, rely on the conversion of a pressure drop inside an atomizer into kinetic energy of an emerging liquid jet or sheet and consequent atomization. They are simple and do not require an additional input of energy or medium however their application is limited to liquids with lower viscosity and they require high input pressures to generate fine spray. Air-assist atomizers overcome these drawbacks. They offer two basic configurations. In the external-mixing configuration, air impinges on the emerging liquid sheet downstream the nozzle. In the internal-mixing configuration, to which effervescent atomizers belong to, air and fuel mix upstream of the exit orifice.

Working principle of effervescent atomizer is clear from Fig. 2.2. A gas is injected with low relative velocity into a liquid flowing through central channel of the atomizer. Gas–liquid two-phase flow is created upstream of the atomizer discharge orifice. The liquid, reaching the

discharge orifice, is transformed by the gas volumes into thin film and ligaments. Gas volumes emerging from the nozzle expand rapidly and disintegrate the liquid into droplets.

Effervescent atomizers are used in numerous engineering applications: combustion (gas turbine combustors, furnaces, boilers and internal combustion engines), industrial painting, spray deposition and spray coating, consumer product sprays, spray drying, agriculture and process industry.

Major advantages of effervescent atomizers according our work [3] are: relative insensitivity to liquid physical properties, ability to provide good atomization over a wide range of operational conditions, large atomizer turn-down ratios, a good atomization at very small gas flow rates [4] and at low injection pressures. The effervescent atomizers have a larger discharge orifice than conventional atomizers, which facilitates fabrication and alleviates clogging problems in atomization of suspensions and slurries. A drawback of effervescent atomization in some applications is the wide distribution of droplets (corresponds to δ of about 2 in Rosin–Rammler distribution [5]. Another complication is the need for separate supply of atomizing air.

2   ATOMIZERS AND EXPERIMENTAL EQUIPMENT

Most of data included in this work were acquired during cold testing of various effervescent atomizers in the Spray laboratory at Energy department, Faculty of Mechanical Engineering, Brno University of Technology. The essential experimental equipment consists of a cold test bench with fluid supply system, a Phase-Doppler Analyzer (PDA) and combined PIV–PLIF system. 1D Dantec PDA was employed to measure time-resolved drop size and velocity and planar single-camera and stereoscopic PIV–PLIF system from TSI was used for measurements of the velocity and liquid concentration distributions.

The spray laboratory is equipped with a cold test rig designed for twin-fluid atomizer operation. The test rig was used in several modifications based on the test requirements. Fig. 2.1 gives an overall view on the test rig with a frame that supports a 3D traversing device for atomizer automatic positioning, oil mist aspiration system, spray collector and optical measurement systems. The test rig was used in three configurations: for operation of twin-fluid atomizers (LHO–air), for testing of tri-fluid atomizers (LHO–LHO–air) and for a suspension spraying. The original cold test bench included the oil supply, pressurized air supply, temperature and pressure sensors, flow meters and control valves. It was equipped with a mixing device to prepare a suspension of solid particles with LHO.

Fig. 2.1 Spray laboratory.

Several effervescent atomizers with different construction were designed for tests. An industrial scale atomizer for high-power oil burners was used in a number of size configurations. A transparent research atomizer served for internal flow studies. The industrial scale atomizer is a single-hole, plain-orifice atomizer of type A (see Fig. 2.2).

The atomizers were studied in the vertical downward position of the main axis and operated with LHO using air as the atomizing medium in the "outside-in" gas injection configuration. The

physical properties of the atomized liquid, LHO, and the atomizing medium, air, are documented in Table 2.1.
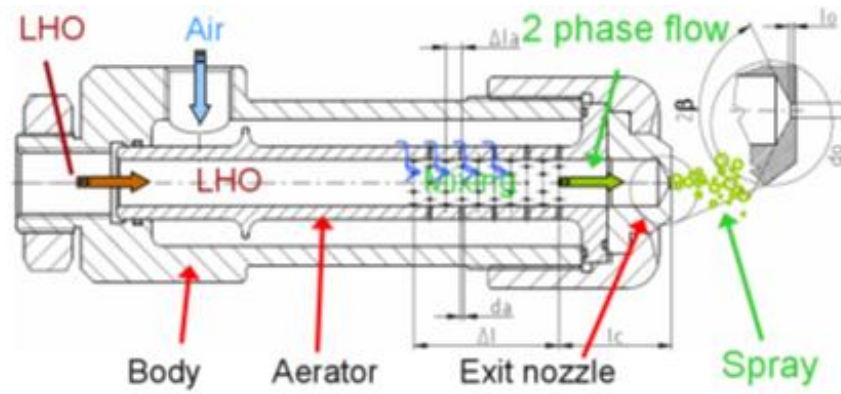
Fig. 2.2 Schematic layout of the research atomizer.

Table 2.1 Physical Properties of Fluids at Room Temperature.

Fluid	μ (kg/m·s)	σ (kg/s^2)	n_r (–)	ρ (kg/m^3)	c (J/kg·K)
LHO	0.0185	0.0297	1.488	874	1850
Air	1.82×10^{-5}	–	1.001	1.23[b]	1005/715[c]
Water[a]	0.0010	0.0727	1.333	1000	4183

[a] reference medium
[b] normal conditions
[c] c_p/c_v

3 INTERNAL TWO-PHASE FLOW AND DISCHARGE

Formation of a two-phase gas–liquid mixture inside the atomizer and its further development prior to the discharge is a process which has direct impact on resulting spray (chapters 4.2.2 and 4.3). The text given here was in a modified form published in our conference papers [6] and [7].

3.1 FLUID MIXING AND INTERNAL TRANSPORT

The atomization process starts with the introduction of gas into the liquid. Interaction between the gas and liquid differs depending on gas-to-liquid mass flow rate ratio (GLR) and moderately also on the input pressure as seen in the Baker's map for the vertical flow (Fig. 3.1). Qualitatively different mixture forms at low GLR and at high GLR [8]. Bubbly flow, present at low GLR, changes to slug, churn, annular and finally to dispersed flow with GLR increase. Flow regime significantly influences the break-up process and resulting spray. We confronted the predicted regimes with results of visualization of two-phase flow inside a transparent effervescent atomizer ([9], chapter Two-Phase Flow Visualization). The calculation of the Baker's map coordinates was compiled into a web application accessible at http://www.tpf-map.ic.cz/.
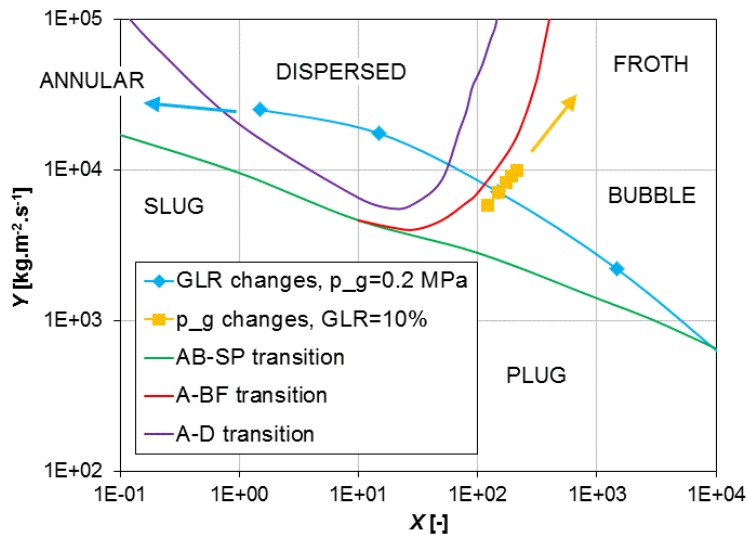

Fig. 3.1 Modified Baker's map for vertical downward two-phase flow with transformed coordinates according to [10]. Arrows show direction of regime change while the appropriate values increase. AB-SP: line defining transition between bubble and plug or annular and slug pattern, A-BF: transition between annular and bubble-froth pattern, A-D: transition between annular and dispersed pattern.

The mixing process is, in the simplest case of equal input temperature of gas and liquid, practically isothermal. Input gas pressure, p_{g1}, differs from the liquid pressure, p_{l1}, only to allow gas to flow through aeration holes; $\Delta p_1 = p_{g1} - p_{l1}$ is typically in kPa rate. Energy related to the pressure difference transforms into heat due to friction losses and into surface energy of the mixture. Small pressure difference along the mixing channel is needed to overcome wall friction and resistance of the turbulent motion of the two-phase mixture. These effects spend only small fraction of the input energy, However the mixture formation is very important for the resulting spray; size of produced droplets is proportional to the square root of the initial thickness or diameter of the ligaments from which they were formed [11].

3.2 DISCHARGE OF GAS–LIQUID MIXTURE

The mixture accelerates due to cross-section reduction which leads to bubble elongation [12, 13] and expansion controlled by the pressure drop. It causes further increase in interfacial surface. Liquid membranes, filaments and ligaments are formed [14]. Gas bubbles expand and finally explode [15, 16] causing ligament thinning and disruption. The gas flows with higher velocity and it acts on the liquid ligaments similar way as in the case of airblast prefilming atomization. This velocity slip results in (1) acceleration of the liquid mass followed with (2) continuing transformation of the bulk liquid into shreds and ligaments and also importantly to (3) a surface wave formation which enhances the atomization process.

We use two analytical models to describe the two-phase discharge and to predict the discharge coefficient of twin-fluid atomizers with internal mixing; the Homogeneous Flow Model (HFM) and Separated Flow Model (SFM) which correspond to the extreme cases of gas–liquid discharge without slip and discharge with maximum slip respectively. Corrections to include effects of fluid physical properties and nozzle geometry to the discharge were added and resulting model has been compared with experimental data for a set of single-hole effervescent atomizers under wide range of inlet gauge pressures and GLRs. A match with $R^2 = 0.95$ was found between the model based and the experimental discharge coefficients. We fully describe the procedure in [3] Appendix 2. The procedure for discharge coefficient estimation containing HFM and SFM was compiled into a free-access web application at http://www.nozzle.ic.cz/.

Character of thermodynamic interaction between gas and liquid during discharge affects the discharge coefficient, C_d. Three cases are considered for both the HFM and SFM: (1) case with isentropic exponent of the two-phase mixture, $k = K$, (2) gas isentropic exponent used (frozen flow, $k = \kappa$) and (3) isothermal expansion of two-phase mixture ($k = 1$) (see Fig. 3.2 left). Discharge coefficients for the HFM and SFM differ up to 3 times and mainly in typical GLR range of operation of twin-fluid atomizers $1 - 100\%$ (Fig. 3.2 right). Momentum transfer between the liquid and gas should then significantly influence the slip between the liquid and gas and finally the liquid C_d. Figs. 3.2 left and right also show very small difference in discharge coefficients for case 2 and 3 when compared with case 1 for the same discharge model. Case 2 gives higher C_d than the case 1 for HFM mainly for GLR = $0.1 - 100\%$ while case 3 gives lower values when GLR > 10%. Differences between the three cases of particular model are less than $\pm 10\%$ in whole the GLR range. It means that there is low influence of the heat interaction between the liquid and gas.
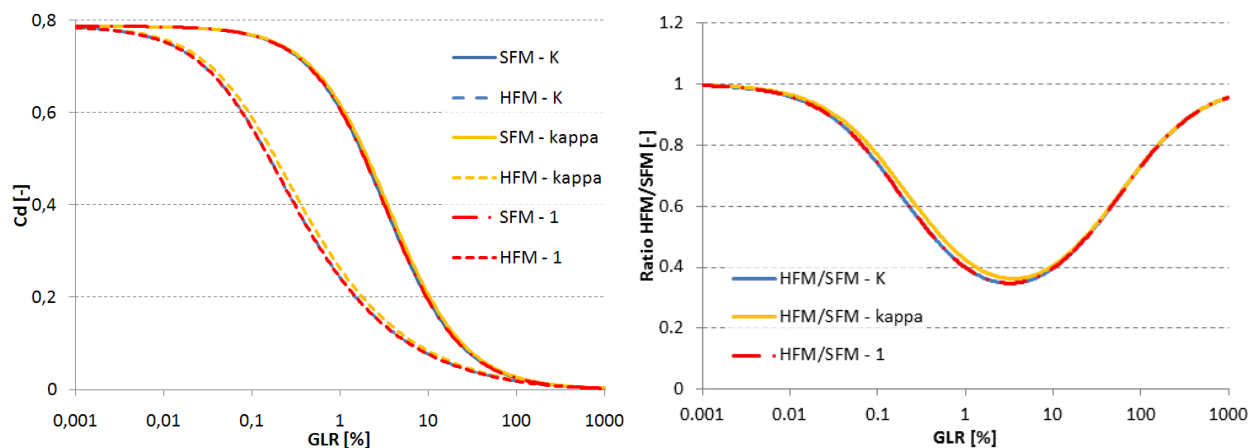

Fig. 3.2 Comparison of C_d for HFM and SFM (left), differences between HFM and SFM (right), discharged fluids: LHO/air, nozzle size: $d_o = 2.5$ mm, $l_o = 0.7$ mm, $\beta = 45°$, $\Delta p = 0.05$ MPa.

4   SPRAY CHARACTERISTICS

Various atomizer applications pose different requirements on the spray characteristics. However several parameters are usually particularly important. The atomized liquid is to be delivered to the target place in specified amount, with certain size range of the droplets and spatial distribution of the liquid. This chapter focuses on general description of the structure of effervescent sprays, spatial distribution of the discharged liquid, size characteristics of droplets and spray steadiness; the material given here was published in our papers [6, 17-19].

Intensity in the momentum transfer between the gas and liquid inside the discharge orifice can be estimated by comparing of real discharge characteristics with predictions by analytical models of two-phase discharge. We have done this comparison in [3] Appendix 2 and have found real discharge coefficient just in the middle of the two extreme cases of gas–liquid discharge: (1) without slip between the gas and liquid phases (HFM) and (2) discharge with maximum slip between the phases respectively (SFM) irrespective of the pressure and GLR. The velocity slip between gas and liquid phase, which is very small for bubbly flow and large for annular flow inside the mixing chamber, increases in the constricted exit orifice. Gas accelerates and reaches the highest velocity in the smallest cross-section for non-choked conditions or near behind it for choked conditions. Momentum transfer between gas and liquid accelerates the liquid; small liquid fragments reach higher velocity than large filaments oriented mostly parallel to the flow. Expanding gas decelerates with distance from exit orifice. Formed droplets keep momentum of the parent liquid fragments so in large distances from the orifice large droplets are faster than surrounding air while velocity of small droplets corresponds to the air velocity. Mixing with surrounding air also decelerates the spray. The discharge process thus results to a temporally and spatially variable velocity, size and concentration distribution of the liquid.

4.1   SPATIALLY AND TEMPORALLY RESOLVED DISTRIBUTIONS OF THE LIQUID

Suitable spatial distribution of the liquid within the spray and its temporal stability are important factors in application areas such as combustion, surface coating and powder generation. In this section we study a spray generated by a simple effervescent atomizer (as described in [9]) continuously operated in the vertical downward position of the main axis on the cold test bench. LHO was atomized, with air as the atomizing medium. The experiments were performed for several air gauge pressures (in the range $0.1 - 0.5$ MPa) and GLR values ($2 - 50\%$). Combined stereoscopic PIV–PLIF system was used for simultaneous planar measurement of the velocity and concentration of the liquid phase in the spray. A set of image pairs of the LIF intensity was processed into instantaneous 3-component velocity vectors of the droplets and the liquid phase concentration in the plane perpendicular to the spray centreline. The velocity and concentration data were processed into temporally mean and fluctuating concentration and mass flux density images that give information on spatial and temporal character of distribution of the liquid within the spray.

Fig. 4.1 (left) documents the half profiles of the radial distribution of the mean liquid mass flux density for air gauge pressure 0.2 MPa. The data are normalized by their respective maximum value to enable comparison. About 90% of the liquid mass is contained in the area of 44 mm in diameter in the case of GLR = 2%. Spray cone angle decreases with increasing GLR; more than 90% of the liquid mass is included inside circle with 29 mm in diameter for GLR = 50%. Results for different air gauge pressures for GLR = 5% are seen in Fig. 4.1 (right). The pressure variation does not show significant influence on the mean liquid distribution.

Radial profiles of the normalized rms (root-mean-squared) fluctuations of the liquid mass flux density are displayed in Fig. 4.2. The fluctuations have a low value near the spray axis and increase with the axial distance showing a peak value near the spray edge. The spray unsteadiness

strongly depends on GLR (Fig. 4.2, left); the fluctuations are low in the case of high GLR and tend to increase with GLR decrease. This can be observed in the entire radial profile. An influence of the air gauge pressure on the fluctuations of liquid mass flux density is not as significant with an exception of the results at 0.1 MPa (Fig. 4.2 right). Overall values of the fluctuations were also correlated with predicted internal two-phase flow patterns. Increase in GLR leads to a reduction of $\hat{\overline{G}}'(x, y)$ and corresponding overall value $\hat{\overline{G}}'$. These results and deeper analysis of the liquid distributions in the spray are presented in [19].
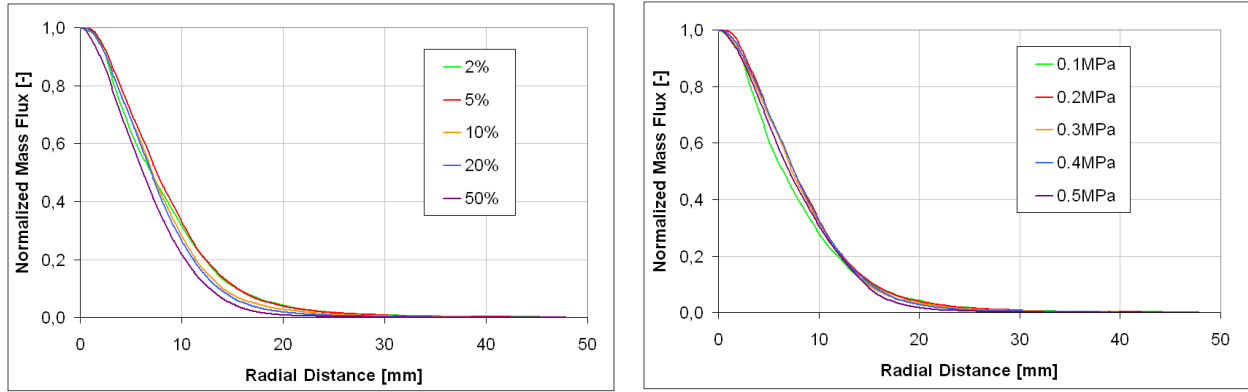

Fig. 4.1 Radial profiles of $\overline{G}(x, y)$ for varying GLR at $p_a = 0.2$ MPa (left) and for varying p_a at GLR = 5% (right).
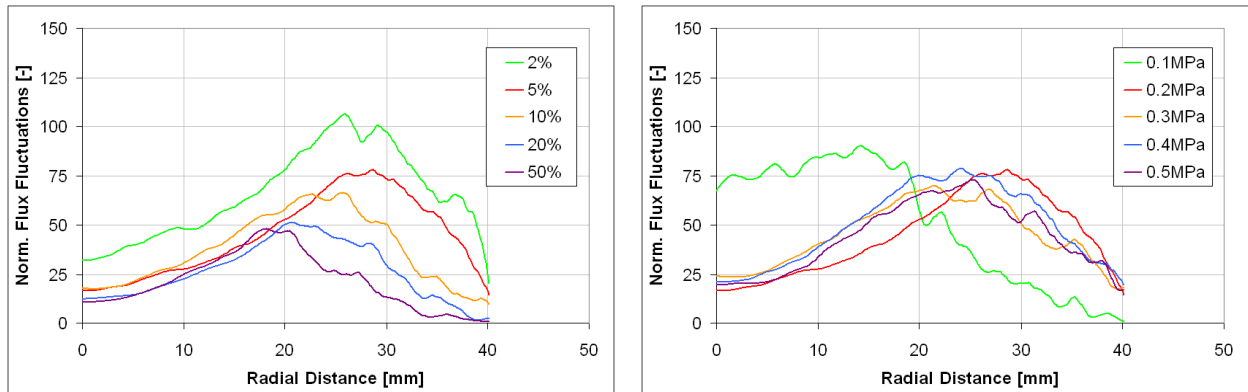

Fig. 4.2 Radial profiles of $\hat{\overline{G}}'(x, y)$ for varying GLR at $p_a = 0.2$ MPa (left), for varying p_a at GLR = 5% (right).

Our next study was undertaken to investigate the effect of atomizer internal design on liquid distribution. It is documented in [18] where spray cone angles are estimated using PIV–LIF for a set of atomizes at a range of atomizing pressures and GLRs.

4.2 DROPLET CHARACTERISTICS

Droplet generation is a statistical process which result can be documented by a droplet size distribution. It can be described as a drop number, surface or volume distribution:

$$f_a(D) = \frac{(dn/dD)D^a}{\int_0^\infty (dn/dD)D^a dD} \tag{4.1}$$

and for cumulative distribution

$$\phi_a(D) = \frac{\int_0^D (dn/dD)D^a dD}{\int_0^\infty (dn/dD)D^a dD} . \tag{4.2}$$

Value $a = 0$ refers to the number distributions, $a = 2$ to the surface distributions and $a = 3$ to the volume distributions. Example of typical drop number distribution curve and corresponding cumulative distribution function is displayed in Fig. 4.3.

We often describe a real set of drops in the spray with a specific size distribution by a single value that determines drop characteristics depending on the field of the spray application. General formula for definition of mean drop diameter is [2]

$$D_{pq} = {}^{p-q}\sqrt{\frac{\sum_{i=1}^m D_i^p \Delta n_i}{\sum_{i=1}^m D_i^q \Delta n_i}} \tag{4.3}$$

where p and q are used for determination of a particular statistical diameter. The most often used are arithmetic mean diameter D_{10} for comparison of disperse systems, surface mean diameter D_{20} e.g. for vaporization studies and volume–surface mean diameter or Sauter mean diameter D_{32} for mass and heat transfer evaluations. Other indicators of spray quality describe a drop size range that covers some specific fraction of the drop volume. Values $D_{v0.1}$, $D_{v0.5}$ (mass mean diameter, MMD), and $D_{v0.9}$ represent a diameter below which volumetric fraction 0.1, 0.5 and 0.9 of the total droplet volume in measurement point occurs. Some of the mean diameters are seen in Fig. 4.3.
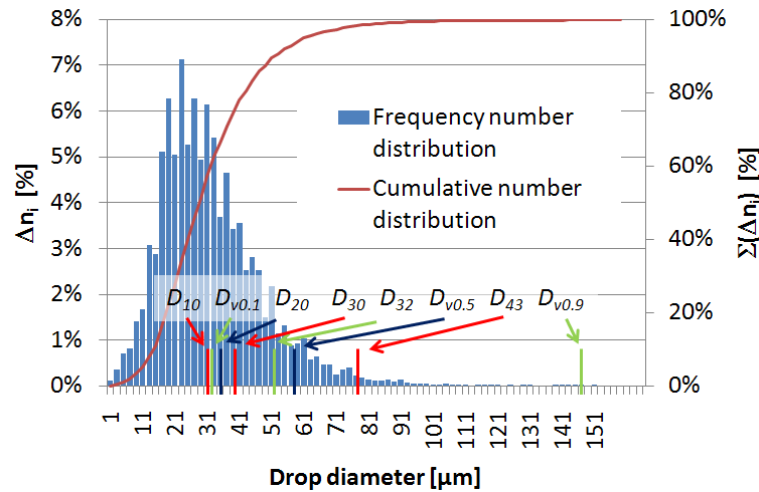

Fig. 4.3 Drop number distribution with marked mean diameters.

Size spectrum of droplets generated by twin-fluid atomizers is not spatially uniform; characteristic diameters vary along the radial distance from atomizer axis (see Fig. 4.9). For the sake of conciseness and comparison of results we defined an integral value of diameter D_{32} (ID_{32}) as a single parameter to represent globally the droplet size. Calculation of the ID_{32} is based on characteristic diameters D_{20} and D_{30} measured at axi-symmetric spray in radial positions r_i with droplet transit frequency f_i using PDA or other point-wise method. Simplified estimation of ID_{32} reads

$$ID_{32} = \frac{\sum_{i=2}^n \left(r_i \cdot D_{30,i}^3 \cdot f_i \right)}{\sum_{i=2}^n \left(r_i \cdot D_{20,i}^2 \cdot f_i \right)} . \tag{4.4}$$

15

Drop size in the spray of effervescent atomizer E2 described in [20] was measured using PDA at pressure 0.1 MPa and GLR 3%. The measurement was performed in the distance 152 mm from nozzle exit in radial positions 0, 5, …., 75 mm from the nozzle axis. Fig. 4.4 shows measured D_{32} and corresponding drop frequency profiles. Volumetric and surface flux densities are calculated according to Eq. (3) and Eq. (7) respectively in [3] Appendix 1. It is seen that maxima of both the flux densities are placed in the spray centreline and gradually decreases. Volumetric flux density multiplied by corresponding area of annulus with mean radius r_i give volumetric flow rate through the annulus. The same stands for the surface flux density. Diameter ID_{32} was calculated using Eq. (4.4) with maximum radius equal to the corresponding abscissa value. The ID_{32} shows moderate increase with radial distance, r_i, up to $r_i \approx 40$ mm and later almost constant value about 64 µm.
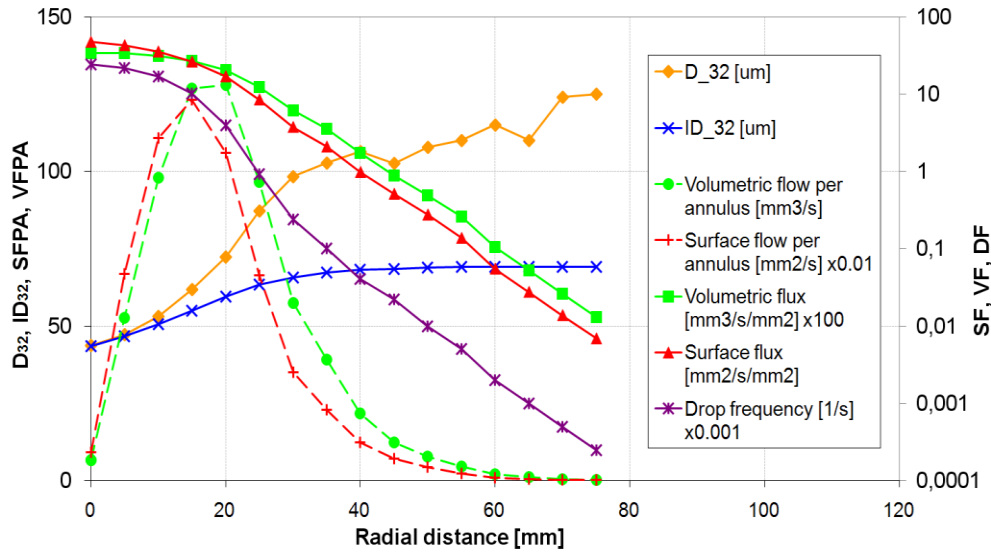

Fig. 4.4 Measured and calculated drop parameters.

Surface diameter D_{20} is important for vaporization studies and it is also used here for estimation of the atomization efficiency (chapter 5.2). D_{20} varies with radial distance similarly as D_{32} so its overall value is required to characterise the spray as a whole. Integral surface diameter ID_{20}, knowing the surface area per time (Eq. (7) in [3] Appendix 1) and corresponding droplet number reads

$$ID_{20} = \sqrt{\frac{\sum_{i=1}^{n} r_i \cdot D_{20,i}^2 \cdot f_i}{\sum_{i=1}^{n} r_i \cdot f_i}} \quad . \tag{4.5}$$

4.2.1 Spatial Distribution of Droplet Characteristics

Fragmentation of the liquid mass under turbulent gas flow is a complex process. Primary and secondary break-up processes followed with droplet agglomeration result in a continuous size distribution. Fig. 4.5 left documents a variation of the size number distribution with axial distance. The results are based on measurements of effervescent sprays using PDA. The distribution is generally similar to log-normal or Rosin–Rammler distribution. The break-up process is almost completed 50 mm bellow the nozzle, so only minor differences are seen between individual curves. Axial velocity distribution (Fig. 4.5 right) resembles normal or log-normal distributions.

Both the maximum and span width strongly depend on the axial distance in the decelerating gas flow.
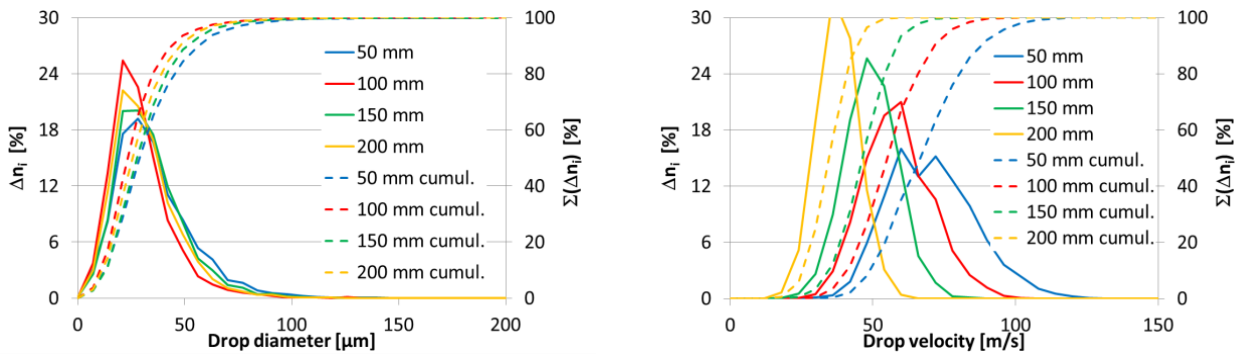

Fig. 4.5 Size (left) and velocity (right) number distributions for atomizer E34 and regime $p = 0.3$ MPa, GLR = 5%, spray centreline.
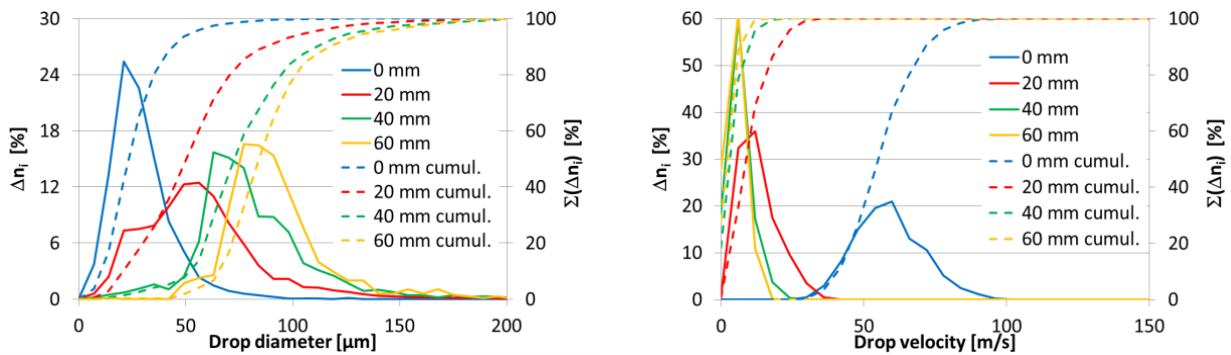

Fig. 4.6 Size (left) and velocity (right) number distributions for atomizer E34 and regime $p = 0.3$ MPa, GLR = 5%, position $z = 100$ mm.
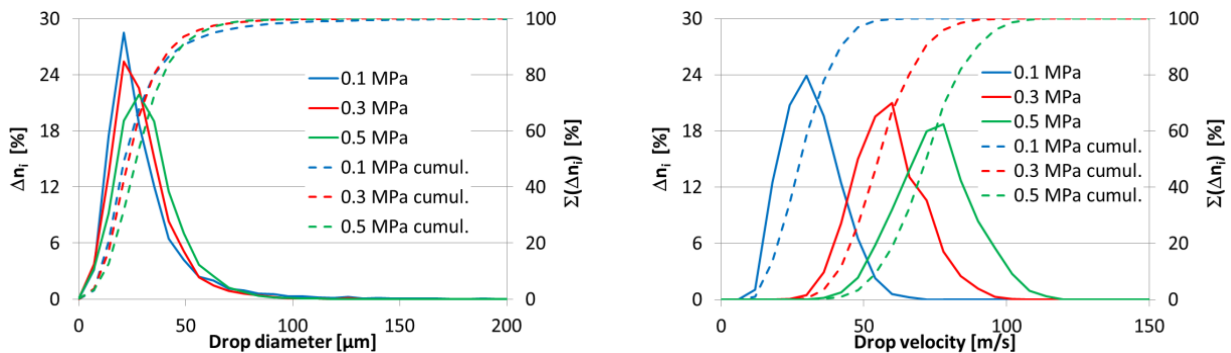
Fig. 4.7 Size (left) and velocity (right) number distributions for atomizer E34 and GLR = 5%, position $z = 100$ mm, $r = 0$ mm.

Droplet size generally increases with radial distance (Fig. 4.6 left). The smallest droplets are generated in the centreline with high initial gas–liquid velocity and high local GLR. While large droplets appear in the spray periphery where velocities drops down (Fig. 4.6 right). Effect of the atomization pressure (Fig. 4.7 left) and GLR (Fig. 4.8 left) on size distributions in the centreline is relatively weak for inspected range of operation conditions, increase in the input energy leads to moderate reduction of droplet size. Much larger effect of operation conditions appears at larger

radial distances as seen in Fig. 4.9. The velocity distributions are always affected significantly as both the pressure and GLR control the discharge velocity (Fig. 4.7 and 4.8 right).

Fig. 4.8 Size (left) and velocity (right) number distributions for atomizer E34 and $p = 0.3$ MPa, position $z = 100$ mm, $r = 0$ mm.

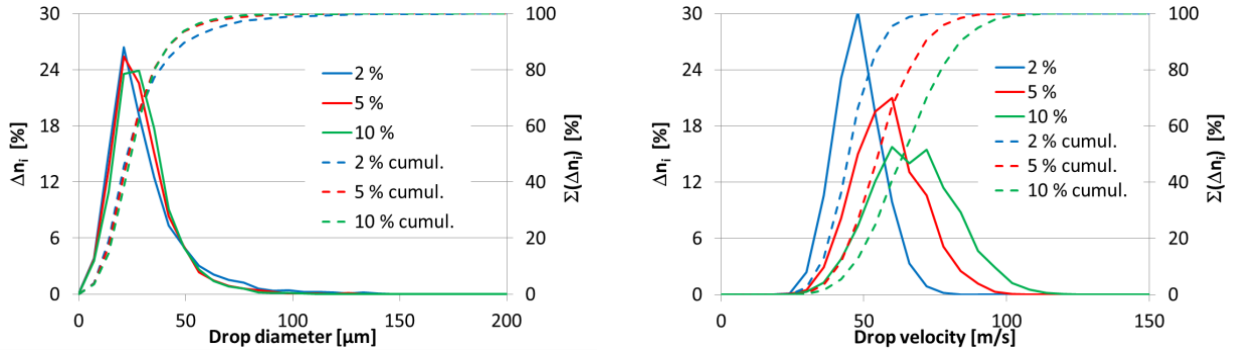Radial size profile (Fig. 4.9) is inversely bell-shaped with a minimum in the centreline where typical values of D_{32} range from 30 to 40 µm. Steep increase in the size in radial distance 10 to 30 mm is followed with relatively constant size profile for larger distances. Larger droplets appear at the edge of the spray. An effect of operation conditions on drop size near the centreline is negligible but for distances larger than 10 mm a negative correlation of size with both the GLR and fluid pressure is evident.
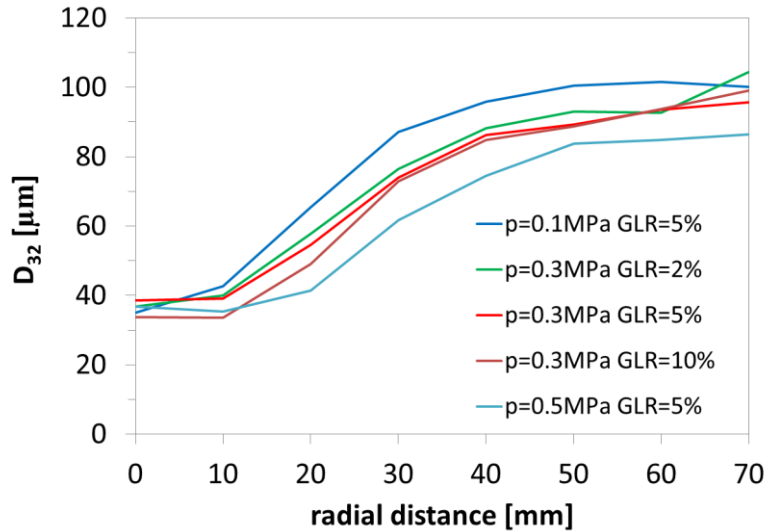
Fig. 4.9 Radial profiles of D_{32} for atomizer E34, position $z = 100$ mm.

To describe the velocity field in twin-fluid spray we start with a simple theoretical case of gas free jet. Spatially resolved velocity according Biswas's and Eswaran [21] is

$$w_g\left(r, z\right) = \frac{\sqrt{3}}{2}\sqrt{\frac{\sigma J}{\rho_g z}}\left(1 - \tanh^2\frac{\sigma r}{z}\right),$$ (4.6)

where $\sigma = 7.67$ and J is total momentum of the jet. Awbi [22] suggests:

$$w_g\left(r, z\right) = \frac{2.47 w_{g0}}{\sqrt{z/d_o}}\exp\left(-6.7\left(\frac{r}{0.1z}\right)^2\right),$$ (4.7)

where w_{g0} is exit centreline velocity and d_o is discharge orifice diameter. Both the equations show the velocity decreases according $1/\sqrt{z}$ and radial velocity profiles are bell-shaped with a maximum in the centreline. Velocity profiles divided by the maximum velocity at given relative radial distance $r_r = r/z$ are identical, so the flow is self-similar with $\hat{w}_g(r_r) = 1 - \tanh^2 \sigma r_r$ according Eq. (4.6) or with $\hat{w}_g(r_r) = \exp(-6.7(10r_r)^2)$ according Eq. (4.7). Note that Panchagnula and Sojka [23] used

$$\hat{w}_g(r_r) = \text{sech}^2(\sigma r_r) \tag{4.8}$$

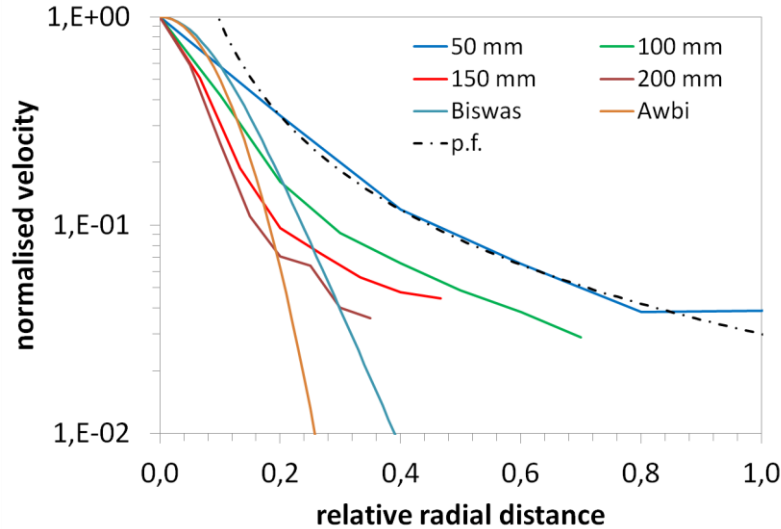as formula for velocity profile of an effervescent spray which is identical to the simplified Biswas equation.

Fig. 4.10 Normalised velocity profiles for atomizer E34 and $p = 0.3$ MPa, GLR $= 5\%$.

Table 4.1 Variation of coefficients a and b with axial distance and with operation conditions for atomizer E34.

| p | GLR | a | | | | b | | | |
MPa	%	50	100	150	200	50	100	150	200
0.1	5	0.026	0.018	0.014	0.0125	-1.3	-1.3	-1.3	-1.3
0.3	2	0.035	0.02	0.012	0.009	-1.4	-1.4	-1.4	-1.4
0.3	5	0.03	0.015	0.009	0.007	-1.5	-1.5	-1.5	-1.5
0.3	10	0.025	0.012	0.0075	0.006	-1.5	-1.5	-1.5	-1.5
0.5	5	0.031	0.014	0.0075	0.0055	-1.55	-1.55	-1.55	-1.55

For description of real velocity field in two-phase jet we will focus on PDA data for axial droplet velocity. Typical normalised velocity profiles at different axial positions are shown in Fig. 4.10. All the profiles are characterised by similar shape however they tend to narrow with increasing axial distance. The profiles are axisymmetric bell-shaped with a maximum in the centreline. Except close the centreline ($r_r < 0.2$) the profiles can be approximated using a power function $\hat{w}_g = a r_r^{-b}$. The coefficient a, varies significantly with axial distance which describes the effect of spray narrowing (Table 4.1). The spray behaves as a jet with its origin shifted by about 200 mm in negative direction. Coefficient b is constant for particular regime and slightly varies with change in pressure and GLR. Velocity profiles defined by Eqs. (4.6) and (4.7) differ

significantly from the measured spray profiles. These profiles are more flat near the centreline however they decline much faster for $r_r > 0.2$.

4.2.2 Effect of Operation Conditions and Internal Geometry on Drop Size

As it has been shown in a number of experimental works [24-31], drop size and velocity in effervescent sprays significantly depend on the input pressure drop and on GLR. Also internal geometry of the effervescent atomizer, given by the dimensions of its mixing chamber and the size and the shape of the discharge orifice, affects the spray quality. To ascertain effect of these factors on industrial scale effervescent atomizer spraying LHO we conducted an experimental study using PDA. Variation of Sauter mean diameter in the spray with operational conditions is described in our work [3], chapter 3. Effect of several geometric parameters (size and number of aerator holes, their location, and the diameter of the mixing chamber) is covered in chapter 4 ibid.

4.3 SPRAY UNSTEADINESS

Despite of good atomization characteristics of internally mixed twin-fluid atomizers several negative issues are known; in particular spray unsteadiness observed under certain operating conditions. The spray unsteadiness (also self-pulsation, sheet fluctuation) is connected with the character of internal two-phase flow. Spray unsteadiness increases with fluctuations in composition of two-phase mixture flowing through the exit orifice (two-phase flow unsteadiness). We have developed a new method for estimation of the two-phase flow unsteadiness and applied it on an effervescent atomizer. Results, acquired under different atomizer operational conditions, show the spray unsteadiness depends mainly on GLR; decrease in GLR causes the spray to become more unsteady. Findings of the new method are complemented and confronted with results obtained by measurement of the spray unsteadiness using Edwards and Marx's method [32]. For detailed description of the work see our paper [9]. Also other method, based on the planar droplet sizing technique, was employed for estimation of spray unsteadiness as described in chapter 4.1. Our method for estimation of the two-phase flow unsteadiness was compiled into a web application for fast and simple evaluation of spray unsteadiness of internally mixed twin-fluid atomizers accessible at http://www.two-phase-flow.ic.cz/.

5   ENERGY CONSIDERATIONS

Atomization of liquids is, from energy point of view, a process of transformation of an input fluid energy into surface energy of produced spray. This process consumes energy and also other important energy related effects are to be considered when designing or choosing atomizer; e.g. transport of the liquid to target position with some required velocity of droplets, impact and air entrainment. Low energy consumption of effervescent atomizers was first noted by Chawla [33]. Here we systematically deal with the energy conversion process in effervescent atomization and compare the atomization efficiency of different atomizer types. Material presented here was in a modified form published in our paper [6].

5.1   GENERAL ENERGY CONSIDERATIONS AND ENERGY RATIOS

Atomization of liquids is a complex energy conversion process accompanied with transformation amongst several energy types. General energy equation (applicable for most of the atomizer types) for steady one-dimensional homogeneous equilibrium flow without mass and energy conservation in some point of an atomizer can be written as:

$$dq + de + di + \frac{dw^2}{2} + gdz - vdp + \sigma da = 0 \qquad (5.1)$$

where q is heat transfer (preheating of high-viscosity liquids and liquids for supercritical or flash-boiling atomization), e is a general symbol for any other input energy source required (electric energy for ultrasonic and electrostatic atomizers, mechanical power for rotary atomizers), i is the mixture enthalpy, g is gravitational acceleration and the term $-v \cdot dp$ is related to the input pressure energy and it also represents an expansion work and the last term characterises a change in the surface area of liquid. The potential energy term ($g \cdot dz$) may be neglected in majority of the atomization techniques and also the terms dq and de are not important for our particular case of twin-fluid atomization of LHO using air in cold (non-reacting) spray considering adiabatic flow conditions. LHO is non-evaporating/non-condensing and the original surface energy of bulk liquid is also negligible. Input energy in pneumatic atomization covers the pressure energy of pumped liquid and pressurised atomizing gas.

Energy ratios in effervescent atomization are documented in Table 5.1 for several sets of input parameters. A share of input energy of compressed gas on the total input energy, e_{pg}, increases with GLR from 88% at GLR = 0.01 to 99% at GLR = 0.1. The input energy is partially transformed into kinetic energy and into surface energy of the internal two-phase flow. Relative kinetic energy of the mixture inside mixing chamber (e_{k1}), with maximum about 0.03% for inlet gauge pressure p_1 = 0.1 MPa and GLR = 0.01, is negligible. Relative surface energy of bubbles/foam inside the mixing chamber, e_{a1}, is in fraction of per cent and decreases with pressure. Fundamental part of the input pressure energy is converted into the kinetic energy of discharged two-phase mixture. It is then partially transferred to the momentum of surrounding gas [34], into expansion work when the gas expands out of the atomizer, and some part also remains with the moving dispersed gas–droplet flow. Kinetic energy of the spray is calculated for data from atomizer E34 (Table 1 in [3]) measured using PDA in axial distance of 100 mm from the exit orifice. Remaining kinetic energy in this distance is already very low. Relative energy of flowing gas is only 0.05% of the total input energy at p_1 = 0.5 MPa and GLR = 10%. It increases with GLR and with input pressure. Relative energy of moving droplets shows opposite tendency with maximum values in units of per cents at low pressures and low GLRs. Small fraction of the input energy is transferred to the increase of droplet surface. Relative surface energy of droplets ($e_{a2} = \eta_a$ = atomization efficiency, addressed in chapter 5.2) depends on pressure and GLR with maximum 0.14% for p_1 = 0.1 MPa and GLR = 1%. Relative expansion work of the gas, a_{e2}, is about 20 − 30% depending on the input pressure. Most of the input energy ends converted to turbulent internal/external flow and mixing of the viscous two-phase fluid, shear and frictional

losses on passage walls, losses during choked discharge and transferred momentum to the surrounding atmosphere.

Table 5.1 Energy balance in effervescent atomization for a set of operation regimes, atomizer operated with LHO and air.

p_1	GLR	e_{pg1} [a]	e_{pl1} [a]	e_{k1} [b]	e_{a1} [c]	e_{kg2} [d]	e_{kl2} [d]	e_{a2} [d]	a_{e2} [e]
MPa	–	%	%	%	%	%	%	%	%
0.1	0.01	88.4	11.6	0.030	0.0111	–	–	0.137	30.5
0.1	0.02	93.9	6.1	0.031	0,0117	0.012	1.229	0.078	32.0
0.1	0.05	97.4	2.6	0.027	–	0.026	0.509	0.035	32.3
0.1	0.1	98.7	1.3	0.021	–	0.033	0.222	0.019	31.2
0.3	0.01	88.4	11.6	0.015	0.0028	–	–	0.074	30.2
0.3	0.02	93.9	6.1	0.012	0.0029	0.035	1.025	0.042	31.8
0.3	0.05	97.4	2.6	0.009	–	0.040	0.381	0.019	32.0
0.3	0.1	98.7	1.3	0.006	–	0.035	0.185	0.010	31.0
0.5	0.01	88.4	11.6	0.009	0.0012	–	–	0.052	25.9
0.5	0.02	93.9	6.1	0.007	0.0013	0.041	0.854	0.029	27.3
0.5	0.05	97.4	2.6	0.004	0,0013	0.048	0.374	0.013	27.5
0.5	0.1	98.7	1.3	0.003	–	0.052	0.194	0.007	26.6

a based on measured data
b calculated using a discharge model proposed in [3] Appendix 2
c calculated for bubbly flow, bubble diameter D_b = 3.5 mm (average value from [9, 16, 35])
d based on PDA results in spray
e calculated for isothermal expansion, energy transfer to the liquid and surrounded air is not taken into account

5.2 ATOMIZATION EFFICIENCY

Atomization efficiency is given by a ratio of the surface energy of droplets in the spray, E_{a2}, to the total input energy E_1 which in twin-fluid atomization consists of energy introduced by the pressurized gas, E_{g1}, and energy of the supplied liquid, E_{l1}. Isothermal compression energy is the minimum necessary one needed to pressurize the gas from atmospheric pressure p_b to the pressure $p_1 = p_{g1} + p_b$ in front of the nozzle. After fragmentation of bulk liquid with volume V_l into droplets having all the same diameter ID_{20} (so called Integral surface diameter) the area of the droplet system will be $A_d = 6 \cdot V_l / ID_{20}$ and the surface energy increase during atomization (neglecting original surface energy of bulk liquid) $E_{ad} = A_d \cdot \sigma$. The atomization efficiency is thus:

$$\eta_a = \frac{E_{a2}}{E_1} = \frac{6 \cdot \sigma / ID_{20}}{p_{l1} + GLR \cdot \dfrac{\rho_l}{\rho_{g1}} \cdot (p_{g1} + p_b) \cdot \ln\left(\dfrac{p_{g1} + p_b}{p_b}\right)} . \tag{5.2}$$

Efficiency of effervescent atomization (shown in Fig. 5.1 left) shows approximately inverse logarithmic tendency with GLR and similarly also with pressure. Increase in the pressure and GLR promotes atomization reducing Sauter mean diameter, D_{32}, as well as D_{20}. However atomization efficiency drops down. Fig. 5.1 right shows that η_a for effervescent atomizers is lower than η_a for pressure atomizers which is in accordance with [2].
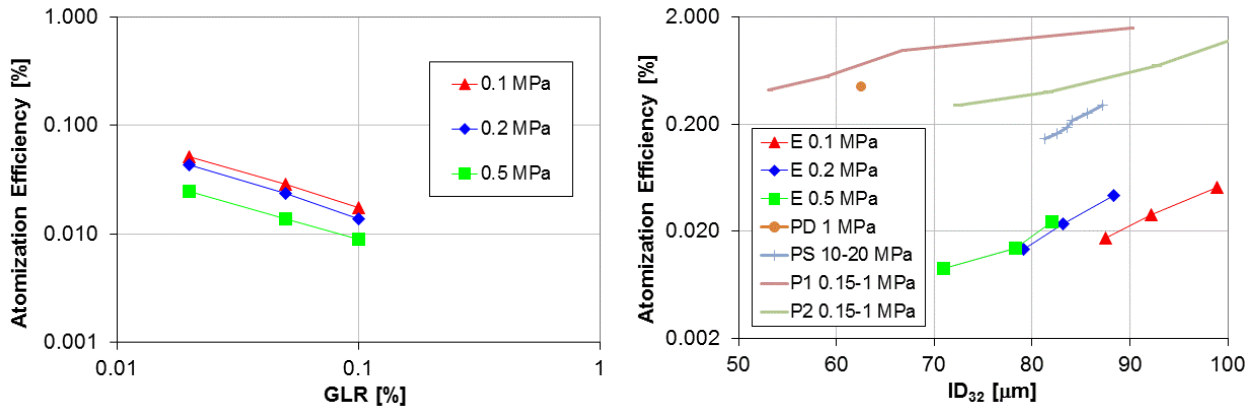
Fig. 5.1 (left) Atomization efficiency of effervescent atomizer at varied operation pressure and GLR. (right) Atomization efficiency of different atomizer types with regard to produced ID_{32}: e – effervescent atomizer with orifice diameter $D_o = 2.5$ mm, operated with LHO/air; PS – pressure-swirl atomizer with $D_o = 2.8$ mm, LHO; PD – simplex atomizer with $D_o = 0.4$ mm, LHO; P1 – new design of pressure-swirl atomizer with $D_o = 0.25$ mm, Kerosene; P2 – old design of pressure-swirl atomizer with $D_o = 0.36$ mm, Kerosene.

6   ATOMIZER DESIGN PROCEDURE

Internal geometry of effervescent atomizers covers several parameters whose optimisation provides fine spray for given operation conditions. We made a systematic study to examine the influence of the atomizer design on the spray performance at variable operation conditions targeting to an industrial LHO burner application. Based on literature review several important parameters were investigated: the size and number of aerator holes, their location and the diameter of the mixing chamber. Their influence on droplet size was studied using PDA at atomizing pressures 0.1, 0.3 and 0.5 MPa and GLR of 2, 5 and 10%. A new procedure for the design of effervescent atomizers, based upon the experimental results and supported by the findings of other authors, was developed. The experimental study and design procedure is fully described in [3]. Main conclusions are as follows:

- operation conditions of the atomizer are defined by the input pressure and by GLR. The increase of GLR significantly reduces the spray drop size. An increase of the operation pressure also leads to finer sprays, but its influence is rather weak.
- The influence of the atomizer design on its performance is moderate. Optimum results can be acquired with the use of a mixing chamber diameter about 4 times the exit orifice diameter. A larger number of aeration holes with smaller diameter leads to a decrease in the drop size.

7 APPLICATIONS

Several effervescent atomizers were designed for specific applications based on requirements from industry. This chapter is focused on description of these atomizers and characterisation of the spray they produce with regard to their usage.

7.1 TRI-FLUID ATOMIZER FOR WASTE FUEL COMBUSTION WITH REDUCED EXHAUST GAS EMISSIONS

Combustion of waste fuels becomes more and more commonplace. The waste liquids often have low heating value, variable physical properties and may contain solid particles which is necessary to account for when selecting an appropriate atomizer. Our task was to design an atomizer for simultaneous atomization of polymer solution and cracked oil. The polymer solution has high viscosity, low heating value and contains particles up to 2 mm in diameter. The oil has higher heating value and is used to assure effective combustion. It is important to enable independent control of both liquid flow rates. The atomizer should be operated under low fluid pressure about 0.2 – 0.3 MPa and should provide a stable spray of good quality to improve combustion efficiency and decrease exhaust gas emissions compared to the current design. High viscosity of the polymer solution and presence of solid particles lead to usage of effervescent nozzle with large exit orifice diameter, placed in the axis of the atomizer. Steam is used as an atomizing medium. The cracked oil is atomized by a multi-hole Y-jet nozzle in a satellite configuration. Results given in this chapter were partially, in a modified form published in our conference paper [36].

7.1.1 Atomizer Design

The demand for a good atomization at low gauge pressure leads to choice of twin-fluid atomizers. Effervescent atomizers enable atomizing liquids with high viscosity and have large discharge orifice to prevent clogging by contained particles, Y-jet atomizers also enable good atomization at low pressure and in contrast with the effervescent atomizers they allow multi-hole construction with uniform distribution of the atomized liquid into particular orifices [37]. Our newly designed atomizer consists of two independent parts (Fig. 7.1). A multi-hole Y-jet nozzle is used for the atomization of the cracked oil. It has an annular passage with 6 exit orifices. Superheated steam is used as an atomizing gas. The polymer solution is atomized using effervescent nozzle in the central part of the atomizer. Steam is injected into the liquid prior to discharge. The two fluids form a mixture, flow downstream and exit the atomizer through an orifice to the ambient atmosphere forming a spray. The exit orifice is 6 mm in diameter to prevent clogging by particles. Quality of the effervescent atomization is relatively independent of variable viscosity and surface tension of the polymer solution used.

7.1.2 Tests

The tri-fluid atomizer was tested on a "cold" test bench with fluid supply system equipped with PDA to characterize the spray quality. LHO was used instead of the polymer solution and air was employed instead of steam. Atomizer operation conditions (fluid pressure, flow rate, temperature) were measured and controlled.

Spray photographs provided at four atomizer loads documented the shape of the individual jets as well as effect of operational conditions on the spray cone angle. An increase of the liquid flow rate caused a moderate enlargement of the spray cone angle. An increase of the atomizing air pressure improved the atomization process and also led to a widening of the spray cone angle of the Y-jet nozzles. The total change of the spray cone angle was from about 65° at low load and low pressure to about 80° at high load and high pressure. Additionally the increase of the

atomizing air pressure improved mixing of the effervescent spray droplets with the droplets from the Y-jet nozzles.
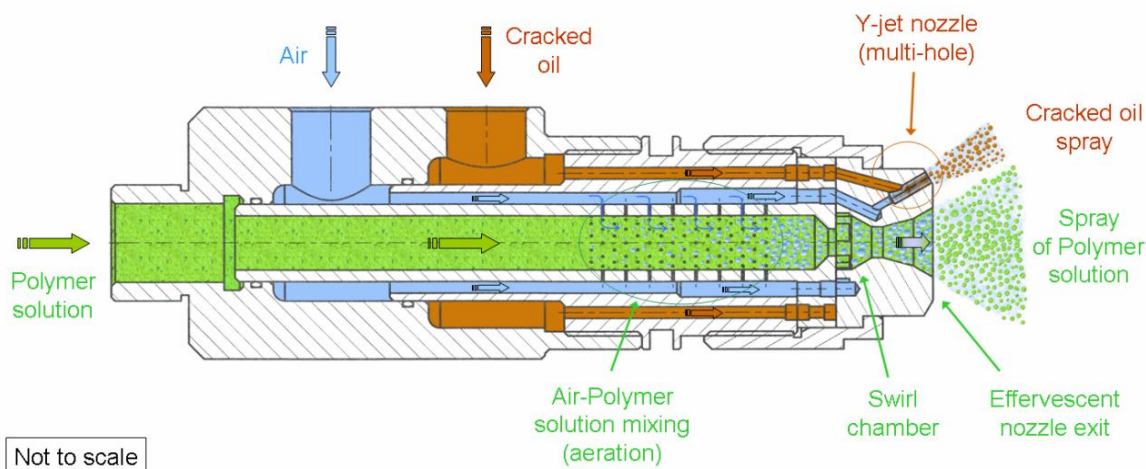

Fig. 7.1 E-Y atomizer cross-section.

The atomizer was also tested in a combustion chamber with polymer solution atomized by effervescent nozzle and cracked oil atomized by the satellite Y-jet nozzles. The tests indicated an improvement of soot emissions in comparison with the current atomizer design. The reduction is $3 - 30\%$ depending on the atomizer operation conditions. NO_x emissions are by $5 - 20\%$ higher than emissions of the old atomizer; these could be reduced without an increase of the soot emissions by optimizing air management of the burner.

The newly developed atomizer gives fine and stable spray for both fuels at low operational pressure and GLR. Tests with polymer solution confirmed feasibility of the choice of the effervescent nozzle for given application. The large exit orifice of the effervescent nozzle prevents clogging by particles contained in the polymer solution. Results of combustion show improved soot emissions compared to the old design and a potential for NO_x reduction.

7.2 SUSPENSION SPRAYING

Effervescent atomizers have larger orifice than conventional atomizers and are thus suitable for spraying of waste liquids (e.g. waste oils) containing solid particles as shown above. Atomization process of suspensions differs from atomization of pure liquids. During the disintegration process the interactions among the three different phases (gas, liquid, solid) as well as the rheological properties of the suspension which depend strongly on the solid particles content, can play an important role. This chapter documents tests of single-hole plain-orifice effervescent atomizer for spraying of waste fuels. LHO loaded with solid particles is used to simulate waste liquids. Results given here were in a modified form published in our conference paper [38].

7.2.1 Atomization of Small-Particle Suspension

Based on results acquired in [3] the atomizer version E35 was chosen for experiments with the suspension. A suspension to substitute the waste liquid was prepared by mixing of LHO with solid particles in specific concentrations. Particles used were Omega–Spheres WSG with density of $0.7 - 0.8$ g/cm^3. Granularity was $10 - 500$ μm and the mean particle size $120 - 150$ μm. Physical

properties of the particles were taken from their technical specification sheets. Suspension of LHO with 5% of the solid particles by mass and pure LHO was atomized.

The test shows that suspension atomization with given mass concentration and particle size through discharge orifice 2.5 mm in diameter is a trouble free process. No clogging or abrasion of the discharge orifice was observed. PDA shown very small difference between size histograms of the LHO and the suspension (Fig. 7.2 left) which suggest the break-up process of the suspension is similar to the break-up of pure liquid. It is in contrast with results of [39] who found important effect of the solids in the suspension. The discrepancy can be explained by lower concentration of solid particles in our case.

The overall effect of the particles on the atomization process is documented in Fig. 7.2 right, where ID_{32}, is compared for a range of GLR. Very similar results for both the cases are seen.
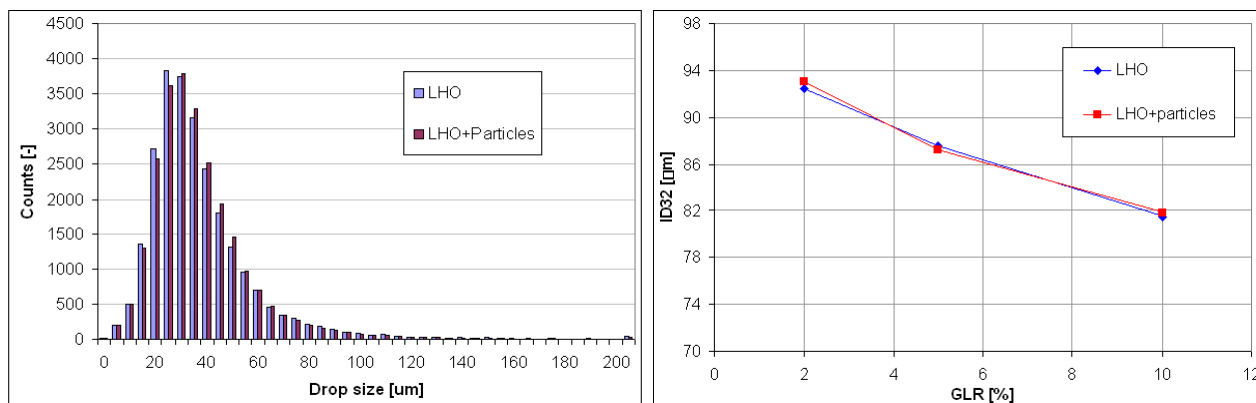

Fig. 7.2 Drop size histogram, $p = 0.1$ MPa, GLR = 5%, radial position 0 mm (left), Integral Sauter mean diameter ID_{32} for LHO and for suspension for varying GLR (right).

7.2.2   Atomization of Suspensions containing Large Particles

Our aim is to develop a twin-fluid atomizer spraying waste liquids (suspensions with a content of large, mm sized, particles) for combustion applications. Such atomiser must produce a fine and stable spray for a required turn-down ratio. Other requirement is a suitable (wide-enough) and preferably also controlled spray cone angle. Large exit orifice and large cross-sections of internal flow channels are required when suspensions containing large particles are used to prevent clogging problems and allow a maintenance free operation.

We designed several atomizers with different geometry of the atomizer exit section. To verify their usability a cold tests with photographic spray observation and droplet size measurement were performed. The waste fuel was simulated using LHO loaded with solid spherical particles. The data given here were presented in conference papers [40, 41].

7.2.3   Design of Novel Pneumatic Atomizers

Effervescent atomizers have large exit cross-section area and produce sprays with substantially wider cone angles than those by plain-orifice pressure atomizers [42]. The spray cone angles vary with inlet pressure and with GLR as well as with atomizer internal dimensions [18]. The cone half-angles of particular atomizers range between 10.5° – 14.4° at GLR 2% and 8.8° – 11.9° at GLR 10% for a range of inlet pressure 0.1 to 0.5 MPa. These values usually are not sufficient for combustion in the furnaces or turbines. Several possibilities to widen the spray cone are known. Whitlow et al. [43] tested an effervescent atomizer with multi-hole and annular orifices. Both the ways lead to reduction of dimensions of the exit orifice cross-section and are not suitable for suspensions containing large particles. Usage of a deflector in the front of the exit orifice enables

good control of spray cone angle but also a risk of choking by carbon. The most frequent way to enlarge the cone angle is an addition of the tangential velocity component to the fluid prior the discharge. It is realised by swirling of a single fluid, gas or liquid, at the atomizer entry, swirling of the two-phase mixture [44] or by an external gas swirler after the discharge [45]. Flat-tangential and helical swirl chamber and swirling inserts were found in the literature [44, 46]. Helical swirl insert was chosen for our application as it allows for a more compact size. Another problem is a presence of large droplets near the spray border which leads to worse exhaust gas emissions. This problem, probably caused by a centralised concentration of the air in the discharged gas/liquid mixture [47], could be solved by an introduction of the secondary air in the exit orifice vicinity from outer side of the emerging spray. Using this information we have designed four new atomizers with modified exit ports and studied their atomization characteristics.

A single-hole, plain-orifice atomizer in the "outside-in" gas injection configuration (labelled as "P" atomizer), designed during our previous work, was used here as a starting point and used also for comparison with the new designs. The former atomizer consists of a cylindrical body with aerator diameter $d_c = 14$ mm. The liquid (suspension) enters the central orifice of the aerator, while the air is injected into the liquid, through a set of $N_a = 40$ holes with diameter $d_a = 1$ mm in the aerator body. Based on the P atomizer its four modifications with swirl in the front of the exit orifice were designed. The parameters l_c, d_c, Δl, d_a and N_a are kept the same for all the atomizers in this study. Exit orifice has always diameter d_o of 3.5 mm and a length l_o of 0.7 mm. Distance of the first row of aeration holes from the discharge orifice is $l_c = 33$ mm for atomizer without swirler and 53 mm for atomizer with swirl insert. The span length, Δl, between the first and the last row is 90 mm.
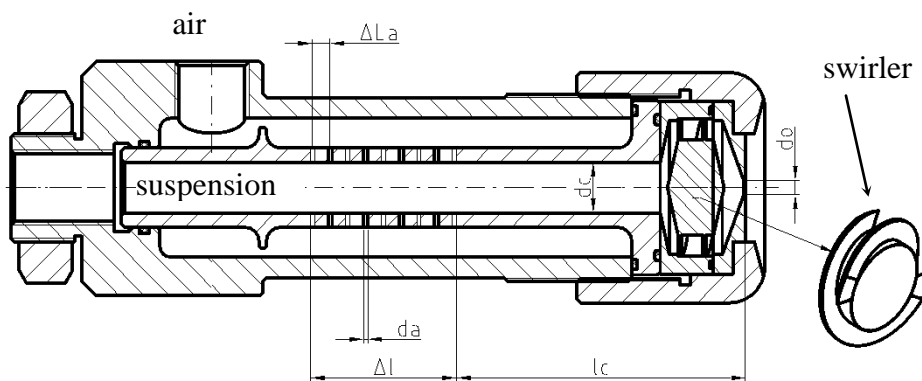

Fig. 7.3 Schematic layout of the atomizer (I, II) with basic dimensions.

Several nozzles were designed and fabricated to test the effect of the swirl chamber on the spray. Three different versions use a simple gas/liquid mixing; the original atomizer without swirler (P) and two modified atomizers with helical swirl insert of different swirling intensity: one atomizer with moderate swirler (I) and one atomizer with intense swirler (II) to extend the spray cone angle, see Fig. 7.3. The atomizer (P) has the aerator connected directly with the exit nozzle. The swirl atomizers have a swirl insert placed between the aerator and the exit nozzle. Swirl insert of atomizer (I) has 4 helical channels with cross-section 5.5×6 mm at mean diameter 32 mm with a pitch 28 mm/thread. Atomizer (II) has 2 channels with cross-section 6×6 mm at mean diameter 32 mm with a pitch 14 mm/thread. Helical swirl ports were chosen as they only moderately enlarge the atomizer size.

Another two atomizers use the internal gas/liquid mixing as the atomizer (P) in a combination with secondary air assistance; one atomizer is constructed with an entry of the swirling secondary

air beyond the exit orifice (III) and the other one with swirling the secondary air at the exit orifice (VI). Primary function of the secondary air is to reduce the droplet size at the spray edge (Fig. 7.4).
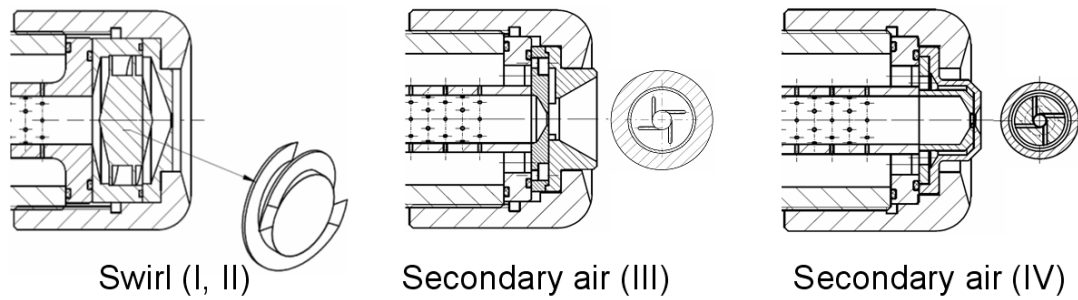

Swirl (I, II)   Secondary air (III)   Secondary air (IV)

Fig. 7.4 Newly designed atomizers.

7.2.4   Results and Discussion

The atomizers were continuously operated on a cold test bench in vertical position of the main axis. Spray cone angles were estimated using spray photography (Fig. 7.5) and droplet size was measured using PDA. The suspension to substitute waste liquids was prepared by mixing of LHO with solid particles in mass concentration 10% of the particles. Particles used were Polystyrene beads with density of 938 kg/m^3, granularity 1.0 – 1.5 mm and the mean particle size 1.2 mm. The particles were practically spherical. Physical properties of the particles were taken from their technical specification sheets. For physical properties of pure LHO see Table 2.1.

Fig. 7.5 Suspension structure at low pressure and low GLR, nozzle with moderate swirler (I).
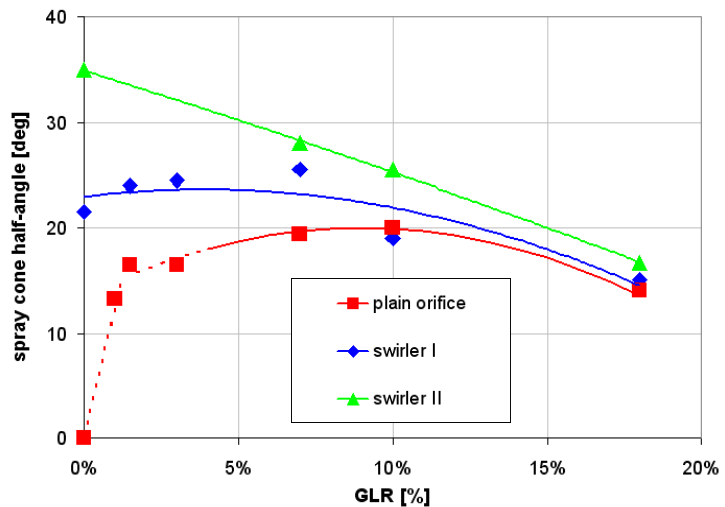
Fig. 7.6 Influence of the mixture swirl and GLR on the spray cone half-angle.

All tests passed with no clogging problems or unsteady or other improper behaviour. It confirms the feasibility of these designs for spraying of suspensions containing large particles. The photographic observation of suspension discharge did not show any agglomeration of the particles in the spray even in the case of elevated concentration of solids up to 50%. The solids are dispersed through whole the spray volume. In the case of higher GLR the particles tend to occur preferably near the spray edge due to their large momentum. The photographs of the spray were used for estimation of the spray cone angle of three atomizers: P, I and II. Influence of GLR and

effect of the swirl intensity on the spray cone angle for all the three atomizers at inlet pressure 0.5 MPa is seen in Fig. 7.6. Atomizer (P) produces a spray with maximum cone half-angle about 20° at GLR 10%. Decrease in GLR leads to a reduction of spray cone angle and to a collapse of the spray cone angle if no air used (GLR = 0). Atomizers (I) and (II) form a spray with wide cone angle already at GLR = 0, where they operate similarly to the pressure-swirl atomizers. Their spray is shaped into a hollow thin conical sheet. Introduction of atomizing air leads to a reasonable increase in the cone angle of the atomizer I, with moderate swirler, up to GLR ≈ 6%. Continuing increase in GLR reduces the cone angle. Spray cone half-angle of atomizer II, with intense swirler, shows a monotonic decrease with increasing GLR. Discharge of pure incompressible liquid differs from the discharge of the liquid–gas mixture. Gas flowing with critical velocity disturbs the angular momentum of the swirled mixture and converts most of the input energy into the axially oriented movement at the exit orifice. Similar behaviour was noticed by other researchers studying internally mixed twin-fluid atomizers with swirl ports [44, 46].

Droplet size in the spray of LHO with air was measured for atomizer P and IV at the distance of 150 mm downstream the exit orifice. Exemplary results of measured radial profiles of Sauter mean diameter, D_{32}, show the inversely bell-shaped course (Fig. 7.7 left) already described in our previous work (chapter 4.2.2). This general tendency is the same for both the atomizers. Atomizer IV gives smaller drops, mainly out of the spray axis, than the atomizer P. It is due to interaction of the liquid with the secondary air at the exit orifice edge.

Overall comparison of the spray produced by the newly designed atomizers is shown in Fig. 7.7 right. The Integral Sauter Mean Diameter, ID_{32}, is calculated for the data measured in radial profiles of D_{32} as shown in Fig. 7.7 left. The secondary air at the exit orifice (IV) gives the lowest ID_{32}, using the same total amount of atomising air. The secondary air beyond the exit orifice (III) (not shown here) did not bring any spray improvement while induced an undesirable contact of the liquid with the conical wall of the exit port.
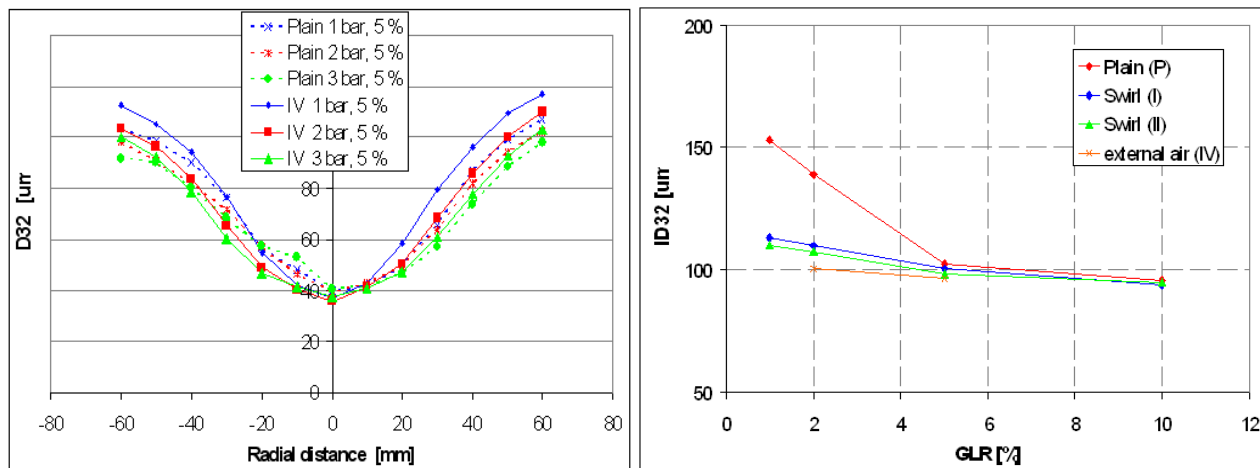

Fig. 7.7 Influence of the air input pressure on ID_{32} for plain-orifice nozzle (P) and the nozzle with secondary air at the exit orifice (IV) at GLR 5% (left); Influence of the GLR 5% on ID_{32} at air input pressure 0.1 MPa (right).

8   CONCLUSIONS

Our work was focused on experimental research of a single-hole, plain-orifice effervescent atomizer with an "outside-in" gas injection configuration for combustion applications. Industrial scale and transparent atomizer versions were designed and fabricated in several modifications. The atomizers were investigated on a cold test bench by means of optical measurement methods.

Internal two-phase flow in mixing chamber of the atomizer was studied first. Wide range of flow regimes were described using the Baker's map for the vertical flow. Two analytical models, the Homogeneous Flow Model and Separated Flow Model, were used for explanation of the discharge and for estimation of discharge coefficient.

Next part of our work was focused on a detailed study of spray morphology using two optical systems. Distribution of the liquid within spray was studied using combined PIV–PLIF technique. Spatially resolved mean distributions of the liquid were found to vary moderately with GLR and weakly also with inlet pressure. RMS liquid distributions indicated temporally unsteady spray behaviour with significant effect of the operation conditions. Spatial distributions of droplet size and velocity were probed by means of PDA. The flow field was found very complex, turbulent and spatially variable. Maximum velocity was found in the spray centreline with approximately Gaussian shape of the radial velocity profile. Size profiles are inversely bell-shaped with the minimum in the spray centreline and the maximums near the spray edge.

Effervescent atomization was considered as an energy conversion process. Our estimation of the energy balance in effervescent atomization shows that the gas/liquid surface formation process during internal mixing as well as during the discharge consumes minor part of the input energy. Most of the input energy is spent to expansion work of the discharged gas, air entrainment process and losses related to the two-phase flow and discharge. Atomization efficiency of effervescent atomizers is found to be in fragments of per cents for common operation pressures and GLRs. The efficiency depends on operation conditions of the atomizer and declines with both the pressure and GLR with approximately logarithmic tendency.

Last part of the work was focused on an application of effervescent atomizers for spraying of waste liquids containing solid particles. Atomization of suspensions (LHO + solid particles) was experimentally studied using PDA. Effervescent atomizers were proved to be suitable for waste liquid spraying due to their relative insensitivity to fuel physical properties and ability to perform a good atomization over a wide range of operating conditions.

9 REFERENCES

[1]   Liu H. Science and engineering of droplets : fundamentals and applications. Park Ridge, N.J. Norwich, N.Y.: Noyes Publications ; William Andrew Pub., 2000.

[2]   Bayvel L, Orzechowski Z. Liquid Atomization: Taylor & Francis Inc., 1993.

[3]   Jedelsky J, Jicha M, Slama J, Otahal J. Development of an Effervescent Atomizer for Industrial Burners. Energy & Fuels 2009;23:6121-30.

[4]   Lefebvre AH. Atomization and sprays. New York: Hemisphere Pub. Corp., 1989.

[5]   Lefebvre AH, Ballal DR. Gas turbine combustion
alternative fuels and emissions. Boca Raton: Taylor & Francis,, 2010; pp. 1 online resource (xix, 537 p.).

[6]   Jedelsky J, Jicha M. Energy Conversion in Effervescent Atomization. 12th Triennial International Conference on Liquid Atomization and Spray Systems. Heidelberg, Germany, 2012.

[7]   Jedelský J, Jícha M. Prediction of Discharge Coefficient of Internally-Mixed Twin-Fluid Atomizers. 24th Annual Conference on Liquid Atomization and Spray Systems. Lisbon, Portugal: Instituto superior Tecnico, 2011; p. 4.

[8]   Shepard TG. Bubble Size Effect on Effervescent Atomization. THE FACULTY OF THE GRADUATE SCHOOL OF THE UNIVERSITY OF MINNESOTA. MINNESOTA: THE UNIVERSITY OF MINNESOTA, 2011; p. 149.

[9]   Jedelsky J, Jicha M. Unsteadiness in effervescent sprays: A new evaluation method and the influence of operational conditions. Atomization and Sprays 2008;18:49-83.

[10]   America PAo. Modified Baker's map for horizontal two-phase flow with transformed coordinates. [online], URL: < http://www.processassociates.com/process/fluid/2faz_xy.htm>, accessed March 2003. 2003 Acessed 2003.

[11]   Lefebvre AH. *Atomization and Sprays*. Bristol: Tailor & Francis, 1989.

[12]   Ramamurthi K, Sarkar UK, Raghunandan BN. Performance characteristics of effervescent atomizer in different flow regimes. Atomization and Sprays 2009;19:41-56.

[13]   Lörcher M, Schmidt F, Mewes D. Flow Field and Phase Distribution Inside Effervescent Atomizers. 9th ICLASS 2003, 2003; pp. 12-9.

[14]   Santangelo PJ, Sojka PE. A HOLOGRAPHIC INVESTIGATION OF THE NEAR-NOZZLE STRUCTURE OF AN EFFERVESCENT ATOMIZER-PRODUCED SPRAY. Atomization and Sprays 1995;5:137-55.

[15]   Linne M, Sedarsky D, Meyer T, Gord J, Carter C. Ballistic imaging in the near-field of an effervescent spray. Experiments in Fluids 2010;49:911-23.

[16]   Gadgil HP, Raghunandan BN. Some features of spray breakup in effervescent atomizers. Experiments in Fluids 2011;50:329-38.

[17]   Jedelsky J, Jicha M. Effervescent atomizer - temporal and spatial variations of spray structure. 10th International Congress on Liquid Atomization and Spray Systems ICLASS-2006. Kyoto, Japan: Institute for Liquid Atomization and Spray Systems - Japan, 2006; p. 8.

[18]   Jedelský J, Landsmann M, Jícha M, Kuřitka I. Effervescent Atomizer: Influence of the Operation Conditions and Internal Geometry on Spray Structure; Study Using PIV-PLIF. 22 Annual Conference on Liquid Atomization and Spray Systems. Como Lake, Italy: Politecnico di Milano, 2008; p. 8.

[19]   Jedelsky J, Jicha M. SPATIALLY AND TEMPORALLY RESOLVED DISTRIBUTIONS OF LIQUID IN AN EFFERVESCENT SPRAY. Atomization and Sprays 2012;22:603-26.

[20]   Jicha M, Jedelsky J, Otahal J, Slama J. Influence of some geometrical parameters on the characteristics of effervescent atomization. Int Conf ILASS Europe 2002. Zaragoza, Spain, 2002; pp. 345-50.

[21]   Biswas G, Eswaran V. Turbulent flows : fundamentals, experiments and modeling. Boca Raton, Fla. New Delhi: CRC Press ; Narosa Pub. House, 2002.

[22]   Awbi HB. Ventilation of buildings. London ; New York: Spon Press, 2003.

[23]   Panchagnula MV, Sojka PE. Spatial droplet velocity and size profiles in effervescent atomizer-produced sprays. Fuel 1999;78:729-41.
[24]   Whitlow JD, Lefebvre AH. Effervescent Atomizer Operation and Spray Characteristics. Atomization and Sprays 1993;3:137-55.
[25]   Sher E, Koren M, Katoshewski D, Kholmer V. Energy consideration and experimental study of effervescent atomizers. Proceedings of ILASS-Europe 2000, 2000; p. Paper II.7.
[26]   Sovani SD, Sojka PE, Lefebvre AH. Effervescent atomization. Progress in Energy and Combustion Science 2001;27:483-521.
[27]   Lefebvre AH, Wang XF, Martin CA. SPRAY CHARACTERISTICS OF AERATED-LIQUID PRESSURE ATOMIZERS. Journal of Propulsion and Power 1988;4:293-8.
[28]   Jedelsky J, Jicha M, Slama J. Characterization of spray generated by multihole effervescent atomizer and comparison with standard Y-jet atomizer. Proc of 9th ICLASS, 2003; p. 0311.
[29]   Chin JS, Lefebvre AH. A DESIGN PROCEDURE FOR EFFERVESCENT ATOMIZERS. Journal of Engineering for Gas Turbines and Power-Transactions of the Asme 1995;117:266-71.
[30]   Lund MT, Sojka PE, Lefebvre AH, Gosselin PG. EFFERVESCENT ATOMIZATION AT LOW MASS FLOW RATES. PART I: THE INFLUENCE OF SURFACE TENSION. 1993;3:77-89.
[31]   Catlin CA, Swithenbank J. Physical processes influencing effervescent atomizer performance in the slug and annular flow regimes. Atomization and Sprays 2001;11:575-95.
[32]   Edwards CF, Marx KD. Multipoint statistical structure of the ideal spray .2. Evaluating steadiness using the interparticle time distribution. Atomization and Sprays 1995;5:457-505.
[33]   Chawla JM. Atomization of Liquids Employing the Low Sonic Velocity in Liquid/Gas Mixtures. Proceedings of the Third ICLASS-85, 1985; pp. LP/1A/5/1-LP/A/5/7.
[34]   Bush SG, P. E. Sojka. Entrainment by Effervescent Sprays at Low Mass Flowrates. *Proc of the 6th ICLASS*, 1994; pp. 609-15.
[35]   Jagannathan TK, Nagarajan R, Ramamurthi K. Effect of ultrasound on bubble breakup within the mixing chamber of an effervescent atomizer. Chemical Engineering and Processing 2011;50:305-15.
[36]   Jedelsky J, Jicha M. Design of Atomizer for Waste Fuel Combustion with Decreased Exhaust Gas Emissions. 31st International Symposium on Combustion. Heidelberg, Germany: University of Heidelberg, 2006; pp. 34-.
[37]   Jedelsky J, Jicha M, Slama J. Characteristics and Behaviour of Multi-Hole Effervescent Atomizers. Proc ILASS-Europe 2004. Nottingham, United Kingdom, 2004; pp. 521–6.
[38]   Jedelsky J, Jicha M, Otahal J. Atomization of Waste Liquids. Proc FLUCOME 2007, 2007; p. 12p.
[39]   Mulhem B, Fritsching U, Schulte G, Bauckhage K. Characterisation of Twin-Fluid Atomisation for Suspensions. Proc ICLASS 2003, 2003; p. 9.
[40]   Jedelský J, Otáhal J, Jícha M. Effervescent Atomizer for Atomization of Suspensions Containing Large Particles. 22 Annual Conference on Liquid Atomization and Spray Systems (Ilass 2008). Como Lake, Italy: Politecnico di Milano, 2008; p. 4.
[41]   Jedelský J, Jícha M. Novel modifications of Effervescent Atomizer, Performance, Advantages and Drawbacks. 23rd European Conference on Liquid Atomization and Spray Systems. Brno: Tribun EU, 2010; p. 5.
[42]   Chen SK, Lefebvre AH. SPRAY CONE ANGLES OF EFFERVESCENT ATOMIZERS. Atomization and Sprays 1994;4:291-301.
[43]   Whitlow JD, Lefebvre AH, Rollbuhler JR. Experimental Studies on Effervescent Atomizers with Wide Spray Angles. Proc AGARD 1993, 1993; pp. 536, 38/1–38/11.
[44]   Karnawat J, Kushari A. Controlled atomization using a twin-fluid swirl atomizer. Experiments in Fluids 2006;41:649-63.

[45]   Dai XF, Lefebvre AH, Rollbuhler J. SPRAY CHARACTERISTICS OF A SPILL-RETURN AIRBLAST ATOMIZER. Journal of Engineering for Gas Turbines and Power-Transactions of the Asme 1989;111:63-9.

[46]   Sankar SV, Robart DM, Bachalo WD. Swirl effervescent atomizer for spray combustion. ASME HTD 1995, 1995; pp. 317–2, 175–82.

[47]   Hampel U, Otahal J, Boden S, Beyer M, Schleicher E, Zimmermann W, Jicha M. Miniature conductivity wire-mesh sensor for gas-liquid two-phase flow measurement. Flow Measurement and Instrumentation 2009;20:15-21.

ABSTRACT

The present work is focused on experimental study of a single-hole, plain-orifice effervescent atomizer with an "outside-in" gas injection configuration for combustion applications. Introductory chapter outlines main features of the effervescent atomization. Next chapter deals with two-phase flow inside the atomizer. Qualitative description of fluid mixing, internal two-phase transport and discharge of the mixture is based on published maps, analytical two-phase flow models are used for predictions of discharge of the gas–liquid mixture and compared with experimental data. Phenomenological explanation of liquid break-up and spray–gas interaction is followed with experimental description of the spray structure using Particle Image Velocimetry – Planar Laser-Induced Fluorescence technique; spatially and temporally resolved distributions of the liquid within the spray and spray cone angles are studied with respect to operation conditions of the atomizer. Spatial variation of droplet characteristics, such size and velocity distributions, are probed by means of Phase-Doppler Anemometry. Energy considerations in effervescent atomization are followed with an estimation of atomization efficiency. The last chapter describes several applications of the effervescent atomizer for waste fuel and suspension spraying.